RADIATION RESEARCH **156**, 594–597 (2001)
0033-7587/01 $5.00

Extrapolation of the DNA Fragment-Size Distribution after High-Dose Irradiation to Predict Effects at Low Doses

A. L. Ponomarev,[a,d,1] F. A. Cucinotta,[a] R. K. Sachs,[b] D. J. Brenner[c] and L. E. Peterson[d]

[a] *NASA Johnson Space Center, Mail Code SN, Houston, Texas 77058;* [b] *Department of Mathematics, University of California, Berkeley, California 94720;* [c] *Center for Radiological Research, Columbia University, New York, New York 10032; and* [d] *Baylor College of Medicine, Houston, Texas 77030*

Ponomarev, A. L., Cucinotta, F. A., Sachs, R. K., Brenner, D. J. and Peterson, L. E. Extrapolation of the DNA Fragment-Size Distribution after High-Dose Irradiation to Predict Effects at Low Doses. *Radiat. Res.* 156, 594–597 (2001).

The patterns of DSBs induced in the genome are different for sparsely and densely ionizing radiations: In the former case, the patterns are well described by a random-breakage model; in the latter, a more sophisticated tool is needed. We used a Monte Carlo algorithm with a random-walk geometry of chromatin, and a track structure defined by the radial distribution of energy deposition from an incident ion, to fit the PFGE data for fragment-size distribution after high-dose irradiation. These fits determined the unknown parameters of the model, enabling the extrapolation of data for high-dose irradiation to the low doses that are relevant for NASA space radiation research. The randomly-located-clusters formalism was used to speed the simulations. It was shown that only one adjustable parameter, *Q*, the track efficiency parameter, was necessary to predict DNA fragment sizes for wide ranges of doses. This parameter was determined for a variety of radiations and LETs and was used to predict the DSB patterns at the *HPRT* locus of the human X chromosome after low-dose irradiation. It was found that high-LET radiation would be more likely than low-LET radiation to induce additional DSBs within the *HPRT* gene if this gene already contained one DSB.

INTRODUCTION

It is known that high-LET and low-LET radiations act differently on DNA because of the differing degrees of spatial clustering of ionizations and DSBs (*1*). DNA fragment size distributions for sparsely ionizing radiations have been described previously by the random-breakage model (*2*). A new DNA breakage model for high-LET radiations has been proposed (*3*). In that work, the focus was on the high-LET component of space radiations, which includes energetic, fully ionized heavy ions. The new model, called DNAbreak, generalized the random-breakage model to incorporate the nonrandom DNA breakage induced by HZE particles (*4*).

To achieve this goal, track structure corresponding to HZE particles is simulated (*5, 6*). This track structure is superimposed on a random-walk chromatin geometry, an approach which produces physically and mechanistically justified DSB patterns in the genome (*3, 7, 8*).

Recent pulsed-field gel electrophoresis (PFGE) experiments at LETs of ≈100 keV/μm or more (*9–11*) measured the corresponding distributions of DNA fragment sizes, where ''size'' is used, here and throughout, to mean DNA content. The ionizations due to one high-LET radiation track are spatially correlated, being predominantly near the line representing the center of the track rather than spread randomly over a whole cell nucleus. Localization of ionizations is determined by the type of incident particles and leads to correlations among DSBs along chromosomes, as opposed to the mostly uncorrected DSBs produced by photons.

Recent PFGE data on the effects of high-LET radiations in mammalian cells include results on larger fragment sizes, ranging from a few kilobase pairs up to about 5.7 Mbp. There are ''globally multiply damaged sites''. The DNA is multiply folded during interphase, but even on a large scale, DNA loci which are separated by fewer base pairs along the DNA contour tend to be closer, at least on average, and neglecting fine structure (*7*). With this kind of geometry, the bias for ionizations to be close to one another in space, at high LET, produces a bias for DSBs to be close to one another along the DNA.

BACKGROUND

The description of the randomly-located-clusters formalism and the Monte Carlo algorithm employed has been given elsewhere (*3, 4, 8, 12, 13*) along with the algorithm validation and benchmarks. The intuitive ideas underlying the randomly-located-clusters formalism are that one track can make a stochastic cluster of DSBs along a chromosome, that different clusters on a chromosome due to different tracks are independent, and that the location of independent clusters in the genome, unlike the nonrandom location of DSBs within one cluster, is random.

The randomly-located-clusters formalism related low-dose, one-track effects to high-dose, multitrack effects, thus making it necessary to sim-

[1] Author to whom correspondence should be addressed at NASA Johnson Space Center, Mail Code SN, Houston, Texas 77058; e-mail: alponoma@ems.jsc.nasa.gov.

ulate only one-track effects. This holds true for various radiations and various chromatin geometries, as long as the spatial distribution of the incident ions traversing a certain area is random. It is assumed that there is no change in LET along the trajectory on the scale of the cell nucleus. The derivation of multitrack effects from one-track effects is conceptually analogous to the convolution formalism for deriving multitrack specific energies from one-track specific energies, but it uses different mathematical methods.

Previous work on the DNAbreak model was done with track structures pertinent to α particles (*3*) or fully charged ions (*13*). It was shown that the DNAbreak model fits the PFGE data better than the random-breakage model for these radiations. In this paper, the effect of HZE particles is compared to that of photons to show explicitly the difference in the effects of high-LET and low-LET radiations on human DNA.

The whole chromosome is located randomly with respect to the track center, with at least some monomers always within the penumbra cutoff radius, which was chosen here to be 15 μm. The radial energy profile is used to calculate the probabilities of having at least one DSB on a monomer, given the monomer location *t*, which is the distance between a monomer and the track center in the *XY* plane (that is, in the plane perpendicular to the direction of radiation). This probability is given by

$$\psi = 1 - e^{-QD(E,A,Z,t)}, \quad (1)$$

where $D(E,A,Z,t)$ is the local dose at a site $t = t_i$ (i is an index for a specific lattice site that has a monomer), and Q is the track efficiency parameter, which controls the probability ψ of creating at least one DSB on a monomer given the magnitude of the local dose $D(E,A,Z,t)$ at a monomer. Here E is ion energy, A is ion mass, and Z is ion charge. In this model, we record at most one DSB per monomer, which is sufficient to define the fragment size up to the lower limit of resolution. The smallest DNA size that can be resolved in this model is about 2 kbp. Note that a monomer can generally have more than one DSB, with QD being the average number of DSBs per locus [from this, the definition of Q follows; see Eq. (2) below]. The unit of Q is Gy^{-1}. All radiochemistry involved in the creation of DSBs by ionizing radiation is encapsulated in the track efficiency parameter Q.

RESULTS

The algorithmic application of the randomly-located-clusters formalism can be expressed by two main equations:

$$Q = \text{DSB\_yield} \times \text{DNA\_size}/N; \quad (2)$$

$$\lambda = DQ/M. \quad (3)$$

Here DNA_size is taken to be 140 Mbp as an average size for a human chromosome, $N = 70{,}000$ is the number of loci that the whole chromosome is divided into, DSB_yield is an empirical DSB yield obtained by a PFGE assay, D is the dose, and M is the average number of DSBs created by one-track action (*8, 13*).

DSB_yield is not determined directly in the experiment: Some approximations are used to infer its value (*9, 11*). If one assumes that the empirical DSB_yield is correct, Q can be determined from Eq. (2). Calculations using the DNAbreak one-track action will determine M (*4*); λ will be determined from Eq. (3). From the randomly-located-clusters formalism, the function for the multitrack fragment-size distribution follows (*8*). This both validates the model and checks for consistency between the fragment-size distribution and the empirical DSB yield.

Another way to use the algorithm is to do a least-squares fit to the fragment-size distribution function with adjustable Q. Note that l will also change as a function of Q (M is also a function of Q, as Q determines the efficiency of radiation in a track). By varying Q, one can obtain the optimized value Q^*, which can be used to evaluate the DSB yield based on the DNAbreak model (Eq. 2).

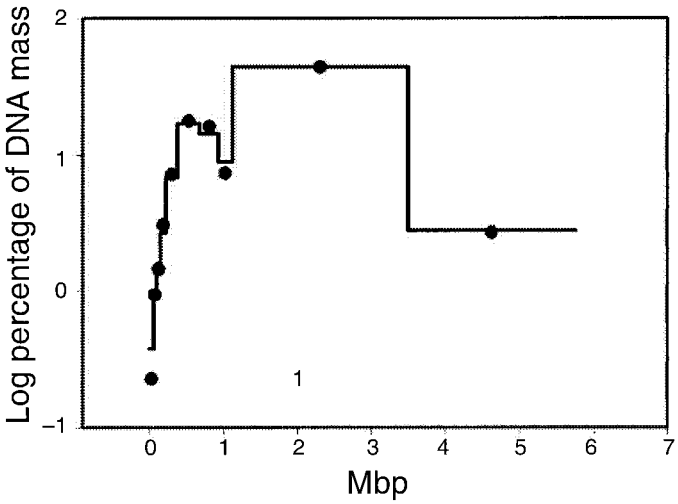

FIG. 1. Comparison of the predictions of the model to the experimental data. The simulated fragment-size distribution function (line) is compared to the PFGE data (circles) obtained by E. Höglund (*11*). The mass fraction of DNA is plotted as a function the fragment size. Human fibroblasts were irradiated with neon ions at 200 Gy and 80 keV/μm. The empirical DSB yield used in the simulation was 8.6×10^{-3} DSB/Mbp Gy^{-1}. The model parameters were estimated as $Q = 1.72 \times 10^{-5}$ Gy, $l = 1.094$ Mbp. The simulated fragment-size distribution function agrees with the data.

Prediction of the Fragment-Size Distribution Function

In Fig. 1, we give an example of the prediction of the fragment-size distribution function by the DNAbreak model based on the empirical DSB yield. The parameters of the model are given in the figure legend. The good agreement between the experimental data and the simulated data indicates the validity of the method: The same DSB yield could result from different distributions. For instance, the model could have predicted a smaller number of small fragments and a greater number of large fragments. A naive estimate of a DSB yield consists of counting fragments as DSBs. A refinement of such an approach would lead to slightly different DSB yields. Hence it can be shown that the empirical DSB yield is closely related to the count of fragments, which could be the same for different distributions.

The observed coincidence of fragment-size distributions shows that the chromatin model and the track structure model are good approximations of the actual tracks and DNA geometries.

Fits of the DNAbreak Model to the PFGE Data

The value of Q can be refined if one does a least-squares fit of the simulated fragment-size distribution function to

TABLE 1
Track Efficiency Parameter

$Q \times 10^5$, 1 Gy	Iron ions (150 keV/μm)	Neon ions 80–97 keV/μm	Neon ions 125 keV/μm	Neon ions 175 keV/μm	Neon ions 225 keV/μm	Helium ions (40 keV/μm)	^{60}Co γ rays (<0.5 keV/μm)
150–200 Gy	3.72[a]	1.70; 2.4[a]	1.72[a]	1.43	1.38[a]	1.83	1.20
100 Gy		1.72	1.78	1.56	1.38[a]	1.67	1.20
50–80 Gy	3.78[a]	1.64	1.78; 1.81	1.44	1.47		
30 Gy			1.78				

[a] Nonoptimized values, inferred from the empirical DSB yield.

the data. Because the model agrees closely with the experimental results, this refinement in Q does not lead to dramatically different values of Q. Parenthetically, we note that because the empirical DSB yields were estimated using some modeling (*9, 11*), the DNAbreak model can be suggested as another tool to derive the DSB yields, using the model fits. These yields follow from the Eq. (2). We do not show new DSB yields here; we only note that they did not differ by more than 5% from the ones estimated previously.

The values of Q for a number of experimental situations are given in Table 1. Based on the construction of the randomly-located-clusters formalism, Q should be independent of dose. The fits also show that Q stays constant for various doses, which again indicates an agreement between the theory and the experiment.

However, the dependence of Q on LET and ion type has not been well understood. For a given ion type, the dependence of Q on LET should be very close to that of the DSB yield. More subtle properties of an ion track, such as the extent of penumbra and dose distribution at a given distance from the ion core, could have an impact on the value of Q. Values of Q obtained from the algorithm presented here could be used to extrapolate from the high-dose data to predict low-dose effects.

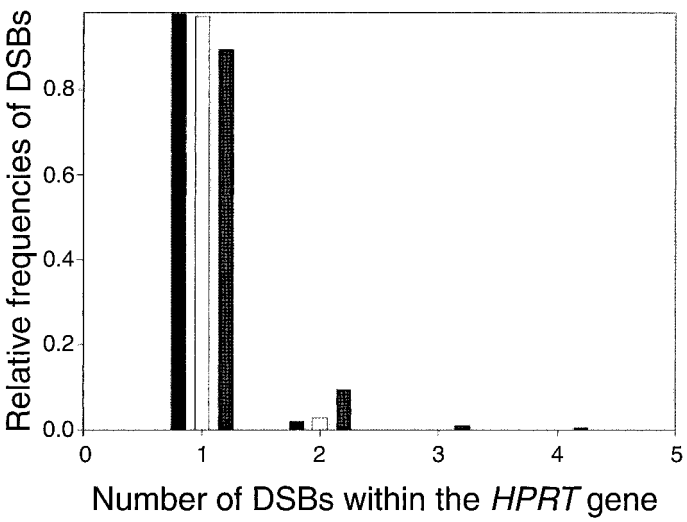

FIG. 2. Damage to the *HPRT* gene after exposure to radiations of various LETs. At low doses (1 Gy), only a small fraction of chromosomes are affected by radiation. To clarify the action of various radiations, we focused on a very small subset of chromosomes, human X chromosomes, in which the *HPRT* gene had been hit, with one resulting DSB. Because of the greater clustering of DSBs after exposure to high-LET radiation, the conditional probability of having more than one DSB within the *HPRT* gene, given that there is already one DSB within the gene, is higher for high LET than low LET. Black columns correspond to ^{60}Co γ rays, <0.5 keV/μm; white columns are for helium ions, 40 keV/μm; and gray columns are for neon ions, 225 keV/μm.

HPRT Gene Damage at Low Doses

Since Q is independent of dose, it is the same for so-called low doses (0–3 Gy) as for high doses. The doses received by astronauts during long space missions (about 100 mGy) fall in this range. At such low doses, a large fraction of cells, as well as chromosomes, are not hit directly. In the range of doses from 10 to 100 mGy, if a chromosome is hit, it is hit by a single track, with a very high probability. Thus one-track action is sufficient to describe the damage to hit chromosomes.

The usefulness of this approach is demonstrated in the data on damage to the *HPRT* gene of the human X chromosome, which is frequently considered in assays of radiation-induced mutations (*14*). If we focus only on those *HPRT* loci (about 45 kbp in size) that were damaged, a conditional probability that there is more than one DSB at the locus, if one DSB is already present, can be calculated with the help of a one-track simulation, and the estimated Q's show the difference between the action of low-LET and high-LET radiations (see Fig. 2). These statistics hold in the low-dose range (0–100 mGy), since only the total number of chromosomes with the affected *HPRT* locus changes, but not the conditional statistics for that small subset of chromosomes.

CONCLUSIONS

The DNAbreak model gives one-track DSB patterns and a systematic way to see what happens when different DSB patterns, from different tracks, overlap on one chromosome or come close to overlapping. The model can be used to extrapolate from the experimental data for high-dose radiations to low doses, where one-track action dominates. This situation is of primary interest for risk estimation for long space missions. The modeling shown here indicates that sparsely and densely ionizing radiations induce different

degrees of damage at a specific locus and that the damage to the human *HPRT* gene, which has been well studied in other radiobiological assays, is more severe for high-LET radiations than for low-LET radiations.

ACKNOWLEDGMENTS

We are grateful to W. Holley and D. Emfietzoglu for discussions. The research was supported by NIH grants RR-11623, CA-49062, CA-77285, CA-24232 and ES-07361, and by DOE Grant FG02–98ER62686 (DJB); by grant DE-FG03-00-ER62909 from the U.S. Department of Energy (RKS); and by the NASA JSC Biophysics Laboratory (ALP, FAC, LEP).

Received: December 28, 2000; accepted: May 18, 2001

REFERENCES

1. H. Wu, M. Durante, K. George, E. H. Goodwin and T. C. Yang, Rejoining and misrejoining of radiation-induced chromatin breaks. II. Biophysical model. *Radiat. Res.* **145**, 281–288 (1996).
2. V. E. Cook and R. K. Mortimer, A quantitative model of DNA fragments generated by ionizing radiation and possible experimental applications. *Radiat. Res.* **125**, 102–106 (1991).
3. A. L. Ponomarev and R. K. Sachs, Polymer chromosome models and Monte-Carlo simulations of radiation breaking DNA. *Bioinformatics* **15**, 957–964 (1999). [Code available at http://www.math.berkeley.edu/~sachs]
4. A. L. Ponomarev, D. J. Brenner, L. R. Hlatky and R. K. Sachs, A polymer, random walk model for the size-distribution of large DNA fragments after high-LET radiation. *Radiat. Environ. Biophys.* **39**, 111–120 (2000).
5. F. A. Cucinotta, H. Nikjoo and D. T. Goodhead, Applications of amorphous track models in radiation biology. *Radiat. Environ. Biophys.* **38**, 81–92 (1999).
6. F. A. Cucinotta, H. Nikjoo and D. T. Goodhead, Model for radial dependence of frequency distributions for energy imparted in nanometer volumes from HZE particles. *Radiat. Res.* **153**, 459–468 (2000).
7. R. K. Sachs, H. Yokota, G. van-den-Engh, B. Trask and J. E. Hearst, A random-walk/giant loop model for interphase chromosomes. *Proc. Natl. Acad. Sci. USA* **92**, 2710–2714 (1995).
8. R. K. Sachs, A. L. Ponomarev, P. G. Hahnfeldt and L. R. Hlatky, Locations of radiation-produced DNA double strand breaks along chromosomes: A stochastic cluster process formalism. *Math. Biosci.* **159**, 165–187 (1999).
9. M. Löbrich, P. K. Cooper and B. Rydberg, Non-random distribution of DNA double-strand breaks induced by particle irradiation. *Int. J. Radiat. Biol.* **70**, 493–503 (1996).
10. H. C. Newman, K. M. Prise, M. Folkard and B. D. Michael, DNA double-strand break distributions in X-ray and alpha-particle irradiated V79 cells: Evidence for non-random breakage. *Int. J. Radiat. Biol.* **71**, 347–363 (1997).
11. E. Höglund, E. Blomquist, J. Carlsson and B. Stenerlöw, DNA damage induced by radiation of different linear energy transfer: initial fragmentation. *Int. J. Radiat. Biol.* **76**, 539–547 (2000).
12. A. L. Ponomarev and R. K. Sachs, Radiation breakage of DNA: A model based on random-walk chromatin structure. *J. Math. Biol.*, in press.
13. A. L. Ponomarev, F. A. Cucinotta, R. K. Sachs and D. J. Brenner, Monte-Carlo predictions of DNA fragment-size distributions for large sizes after HZE particle irradiation. *Phys. Med.* **17** (Suppl. 1), 155–159 (2001).
14. E. A. Leonhardt, M. Trinh, H. B. Forrester, R. T. Johnson and W. C. Dewey, Comparison of the frequencies and molecular spectra of HPRT mutants when human cancer cells were X-irradiated during G_1 or S phase. *Radiat. Res.* **148**, 548–560 (1997).